sustainability

MDPI

Article

Novel MPPT Controller Augmented with Neural Network for Use with Photovoltaic Systems Experiencing Rapid Solar Radiation Changes

Ahmad Dawahdeh [1,*,†], Hussein Sharadga [2,†] and Sunil Kumar [2]

[1] Department of Mechanical Engineering, Jordan University of Science and Technology, Irbid 22110, Jordan
[2] Department of Mechanical Engineering, Texas A&M University, College Station, TX 77843, USA; hssharadga@tamu.edu (H.S.); ksunil@tamu.edu (S.K.)
* Correspondence: aidawahdeh@just.edu.jo
† These authors contributed equally to this work.

Abstract: A maximum power point tracking (MPPT) controller optimizes power harvesting in photovoltaic (PV) systems under varying conditions. The perturb and observation (P&O) algorithm is commonly used for MPP tracking, but suffers from slow response, loss of tracking direction, and entrapment. The current research proposes a neural network (NN) integrated with the P&O algorithm to enhance tracking performance during sudden variations in solar irradiance. The proposed neural network updates the duty cycle change when detecting sudden changes. It effectively estimates the duty cycle change even when trained with a small dataset. The integration between the NN and P&O significantly improves tracking performance compared with the conventional P&O algorithm, especially under sudden irradiance changes.

Keywords: MPPT controller; perturb and observation; PV system; neural network; prediction

check for updates

Citation: Dawahdeh, A.; Sharadga, H.; Kumar, S. Novel MPPT Controller Augmented with Neural Network for Use with Photovoltaic Systems Experiencing Rapid Solar Radiation Changes. *Sustainability* **2024**, *16*, 1021. https://doi.org/10.3390/su16031021

Academic Editor: Fernanda Strozzi

Received: 13 December 2023
Revised: 14 January 2024
Accepted: 17 January 2024
Published: 25 January 2024

Copyright: © 2024 by the authors. Licensee MDPI, Basel, Switzerland. This article is an open access article distributed under the terms and conditions of the Creative Commons Attribution (CC BY) license (https://creativecommons.org/licenses/by/4.0/).

1. Introduction

In the past two decades, there has been a significant increase in energy consumption, leading to a greater emphasis on renewable energy technologies. Solar photovoltaic (PV) systems have gained widespread popularity for generating electricity from solar energy. Extensive research has been conducted to improve the electrical conversion efficiency of solar cells, but the limitations of silicon materials impose constraints on their maximum efficiency. Researchers are exploring new semiconductor materials, but these new materials have a higher cost compared with silicon [1]. Another crucial area of research concentrates on controlling the rate of energy generation by improving MPPT algorithms. These algorithms guide the PV modules to operate at their optimal performance. Improving the MPPT algorithm has been demonstrated as a cost-effective method for boosting both energy productivity and reliability in PV systems [1,2].

The perturb and observation (P&O) algorithm is a widely adopted tracking method for commercial PV systems due to its simplicity and cost-effectiveness, as it can be implemented using inexpensive electrical devices. However, the P&O algorithm is hindered by slow response times and may make incorrect decisions during rapid changes in solar irradiance. The issues in the P&O algorithm can result in suboptimal operation and deviating from the maximum power point. To overcome P&O algorithm limitations, researchers have proposed various modifications to enhance the algorithm's performance. Abdel-Salam et al. [3] suggested a P&O controller for PV systems capable of handling various types of radiation changes such as slow and step changes. The controller was able to track the MPPT with up to 400 W/m^2 rapid change in the solar irradiance. Further, an adapted P&O algorithm has been presented to address an issue observed in the conventional P&O method, a problem arising from the incorrect adjustment of the duty cycle

in response to the initial change in solar irradiance [4]. Harrag et al. introduced a novel P&O approach featuring dynamic adjustments to the duty cycle step size [5]. The method incorporates a proportional-integral-derivative (PID) controller where the parameters are constantly optimized using a genetic algorithm [5]. An evaluation and comparative analysis of the performance of four P&O MPPT controllers were conducted, all of which employed variable step sizes as proposed by Chen et al. [6].

PV performance can be optimized by using optimized tracking systems such as adaptive fractional tracking controllers [7,8], trajectory tracking controllers [9], or MPPT controllers [10]. Various MPPT controllers have been proposed and tested for PV applications aside from the P&O algorithm. Li et al. [10] proposed a fuzzy logic MPPT controller to capture the maximum available power of a PV cell system, where the controller used the beta method to reduce the oscillations of a PV system under fast fluctuations in temperature and solar radiation. Metry et al. [11] employed predictive control that eliminated the need for the current sensor used in the P&O algorithm for tracking the MPP of PV systems. Fathabadi suggested utilizing power slopes to determine proximity to the MPP and adjust the duty cycle step size accordingly [12]. The controller has five-step size values ranging from 0.001 to 0.1 based on slope thresholds [12].

To overcome the limitations of P&O algorithms in handling partial shading conditions, researchers have explored metaheuristic searching algorithms to track the global maximum power point (MPP) in PV systems. A grey wolf optimization proposed by Mohanty et al. showed superior performance compared to P&O in tracking the global MPP, and its robustness was experimentally verified [13]. Mohanty et al. proposed another algorithm by combining the grey wolf algorithm with the traditional P&O to track the global MPP of PV systems [14]; after the wolves get closer to each other, the controller initiates the second stage of tracking which uses the classical P&O algorithm. Sundareswaran et al. combined particle swarm optimization (PSO) with P&O in a two-stage tracking approach to ensure MPP operation under partial shading conditions [15]. Rezk et al. evaluated the tracking performance of two meta-heuristic algorithms—particle swarm optimization, and cuckoo search—for MPPT in PV systems [16]. An improved chaotic particle swarm optimization algorithm was proposed by Pal et al. for MPP tracking under partial shading [17]. Mirza et al. suggested slime mould optimization and improved salp swarm optimization algorithms could be applied to track the MPP in PV systems experiencing partial shading [18].

The P&O algorithm exhibits a slow response and often loses the correct tracking direction during rapid changes in solar irradiance. Valenciaga et al. combined a PI controller with a second order sliding mode observer to address such P&O algorithm problems [19]. The proposed controller succeeded in tracking the MPP during a rapid change in operating conditions [19]. Abdelhamid et al. demonstrated that a new incremental conductance of variable step size proved to have a fast response to sudden changes in solar irradiance [2]. An improved sliding model controller has also been investigated under a 500 W/m^2 sudden reduction in solar irradiance [20].

Neural networks (NN) have been utilized to improve the tracking of the maximum power point; the NN estimates the MPP voltage by training it with solar irradiance and temperature as input variables [21]. Amrouche et al. [22] improved the response of a P&O controller using NN, where the difference between NN output and the real point indicated changes in operating conditions relative to reference values. An approximate equation updated the required change in array voltage [22]. The authors of [23] describe using NN to determine the tracking direction for the P&O algorithm in PV cell applications. NN inputs were voltage and power changes, while the NN output signified the sign of the required duty cycle change (+1 or −1).

To highlight the novelty of this research, an intensive review was conducted on the fuzzy logic and NN used for MPPT tracking. Table 1 summarizes the research conducted on intelligent methods for tracking the maximum power point (MPP) in solar PV systems. Fuzzy logic and NN models were trained using various inputs.

Table 1. Summary of the inputs and outputs used to train different intelligent methods.

Fuzzy Logic			
Reference	**Inputs**	**Output**	**Notes**
[24–27]	$E(K) = \frac{\Delta P}{\Delta I}$ $CE(K) = E(K) - E(K-1)$	ΔD	
[28–35]	$E(K) = \frac{\Delta P}{\Delta V}$ $CE(K) = E(K) - E(K-1)$	D	In [29], the fuzzy is ANFIS-based. In [33] and [34], fuzzy logic is optimized by using GA. In [35] the controller is adaptive.
[36]	$\frac{\Delta P}{\Delta V}$ $\Delta D\ (K-1)$	$\Delta D\ (K)$	
[37]	$\frac{\Delta P}{\Delta V}$ ΔP	ΔV (Size of perturbed voltage)	
[38]	$\Delta P, \Delta V$	ΔV (Size of perturbed voltage)	Particle swarm optimization algorithm optimized fuzzy logic.
[39]	$E(K) = \frac{\Delta I}{\Delta V} + \frac{I}{V}$ $\Delta\ E = E(K) - E\ (K-1)$	$D(K)$	
[40]	$\frac{\Delta I}{\Delta V}$ $\frac{I}{V}$	ΔD	
[41]	$E(K) = \left\lvert \frac{\Delta I}{\Delta V} + \frac{I}{V} \right\rvert$ $\Delta D\ (K-1)$	$\Delta D(K)$	
[42]	$E(K) = \tan^{-1}\left(\frac{\Delta I}{\Delta V}\right) + \tan^{-1}\left(\frac{I}{V}\right)$ $\Delta E = E(K) - E\ (K-1)$	ΔD	
[43]	$E(k) = D(K)\ \Delta VPV\ (K) + \Delta D(K)\ VPV(K)$ $\Delta E = E(K) - E\ (K-1)$ Where: $\Delta VPV\ (K) = VPV\ (K) - VPV\ (K-1)$	$\Delta D(K+1)$	current sensorless
[44–47]	power (ΔP_{PV}) and voltage (ΔV_{PV}) variations or power (ΔP_{PV}) and current (ΔI_{PV}) variations	ΔD, or changes in the reference voltage ΔV	
[48]	(ΔP), (ΔV), and β	ΔD	$\beta = l\ n\left(\frac{I}{V}\right) - c\ V$ C is a function of cell number, cell temperature, and PV module type
[49]	(ΔP) and (ΔI)	ΔD	
[50]	$E_{PI} = \Delta P \times \Delta I$ $\delta\ E_{PI} = E_{PI}(K) - E_{PI}\ (K-1)$	I_{MMP}	
[51]	$G,\ T$	$D,\ V_{mpp}$	ANFIS-based
Neural Network			
Reference	**Inputs**	**Output**	**Notes**
[23]	$\Delta P\ ,\ \Delta V$	1 or −1 (increase or decrease of the duty cycle)	
[21,52–54]	$G,\ T$	V_{MMP}	In [21], NN configuration is optimized using GA. In [52], three trained NNs. NN is selected based on the weather conditions (cloudy, normal, sunny, etc.)
[55]	$G,\ T$	V_{MMP} I_{MMP} P_{max}	Fuzzy is used to find ΔD. Inputs are $E(K) = VMMP - V(K)$, $CE(K) = E(K) - E(K-1)$

Table 1. *Cont.*

Neural Network			
Reference	**Inputs**	**Output**	**Notes**
[56]	$G,\ T$	V_{MMP} I_{MMP}	
[57]	$G,\ T$	I_{MMP}	
[58]	$G_{MPP},\ V_{GMPP}$	D	under partial shading conditions
[59]	G	D	
[60,61]	$G,\ T$	D	
[62–64]	$E(K) = \frac{\Delta P}{\Delta V}$ $CE(K) = E(K) - E(K-1)$	D	In [62], a comparison between NN, ANFIS, Fuzzy, and Fuzzy optimized by use of GA was conducted.
[65]	$E1,\ E2,\ E3$, and $E4$ are the average of incoming irradiance levels on a group of modules	V_{MMP}	under partially shaded conditions
[66]	$I,\ V$	V_{MMP}	
[67]	$I,\ V$	The perturb size for PI controller	
[68]	$G,\ T,\ I,\ V$	I_{MMP}	
[69]	$T,\ I,\ V$	V_{MMP}	
[70,71]	Short-circuit current	D	
[72]	$G,\ T$	V_{MMP}	G is estimated using different NN with I and V as inputs.
[73]	$G,\ T_a,\ V$	D	

Compared with a regular P&O controller, the innovation of the current work is in proposing a novel P&O MPPT controller augmented with an NN for PV cell applications under sudden solar irradiance variation. The proposed controller utilizes the NN as an estimator to swiftly update the first step change in the duty cycle when sudden changes in solar irradiance occur. Thus, the controller ensures rapid adjustments of the duty cycle in response to rapid variations in solar irradiance. While most control systems typically necessitate inputs from multiple sensors to effectively track the maximum power point (MPP), as illustrated in Table 1, the suggested controller exhibits the ability to achieve precise tracking with only a single current sensor. It is the first controller that uses just the current reading for effectively tracking the MPP. It has also been simulated under a wide range of operating conditions, affirming its robustness and effectiveness.

2. P&O Controller

A Neural Network (NN) is a computational system modeled after the biological neural networks found in human brains. It possesses the ability to learn intricate relationships between inputs and outputs, enabling it to serve as a powerful tool for approximating and predicting new outputs based on a given set of inputs. In this study, an NN was implemented to estimate the necessary adjustment in the duty cycle when a PV system experiences sudden fluctuations in solar irradiance. The objective was to use the NN as a supportive tool to enhance the tracking performance of the P&O controller. The proposed NN focuses on estimating the required change in the duty cycle (ΔD_m).

2.1. P&O Integrated with Neural Network

Figure 1 illustrates the relationship between the power, current, and voltage of the solar array and the duty cycle of the voltage converter. It can be seen that an increase in

solar irradiance led to an increase in the duty cycle of the maximum power point (ΔD_m). For example, as the solar irradiance increased from 500 to 1000 W/m^2, the needed ΔD_m. was 0.21. Having a ΔD_m equal to 0.21 is large compared with the fixed 0.0005 that is used in a conventional P&O controller. As a result, the traditional P&O algorithm necessitates a certain amount of time to adapt the duty cycle and attain MPP operation when faced with abrupt shifts in solar irradiance. To address this issue, an NN was employed in the proposed controller to rapidly adapt the duty cycle under sudden variations in solar irradiance. The NN was utilized to estimate the necessary ΔD_m. The values of ΔD_m were 0.21, 0.13, and 0.08 when the solar irradiance changes from 500 to 1000 W/m^2, from 500 to 750 W/m^2, and 750 to 1000 W/m^2, respectively.

The current of the MPP (I_m) changed by 36.11 when the solar irradiance increased from 500 W/m^2 to 1000 W/m^2, and changed by 18.18 and 17.93 when the solar irradiance changed from 500 to 750 W/m^2, and from 750 to 1000 W/m^2, respectively. Hence, the ΔI_m and ΔD_m depend on both the solar irradiance variation (ΔG) and the prior value of the solar irradiance (G). The value of ΔI_m was significant compared to MPP voltage (ΔV_m). The results show that as the current of the PV array increased, the duty cycle increased, and the voltage decreased.

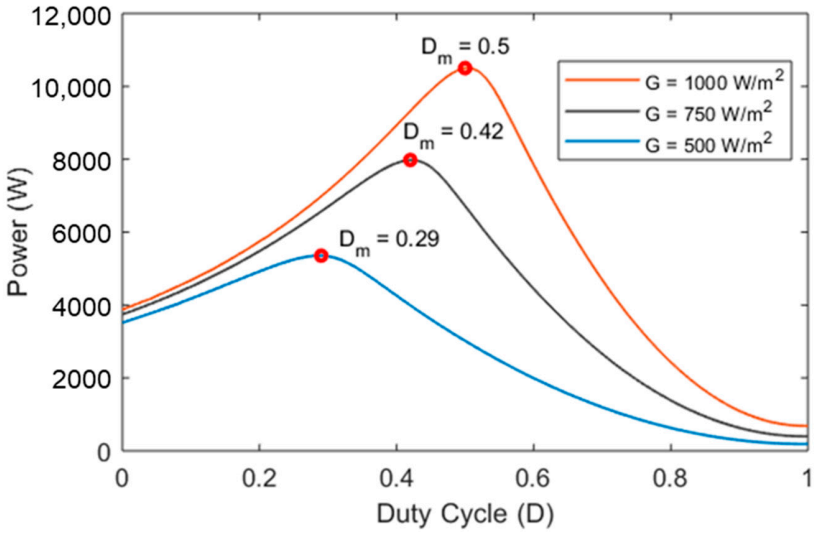
To sum up, the current at the maximum power point (I_m) primarily depends on the solar irradiance (G). Likewise, the duty cycle of the maximum power point (D_m) primarily depends on solar irradiance (G). The MPP duty cycle variation (ΔD_m) depends on both the variation in the solar irradiance (ΔG) and the prior value of (G). Similarly, the MPP current change (ΔI_m) depends on the difference between the radiation reading (G) and the difference in the solar irradiance (ΔG). The described relations are presented as follows:

$$D_m = f\,(G),\ \Delta D_m = f\,(G,\ \Delta G) \tag{1}$$

$$I_m = f\,(G),\ \Delta I_m = f\,(G,\ \Delta G) \tag{2}$$

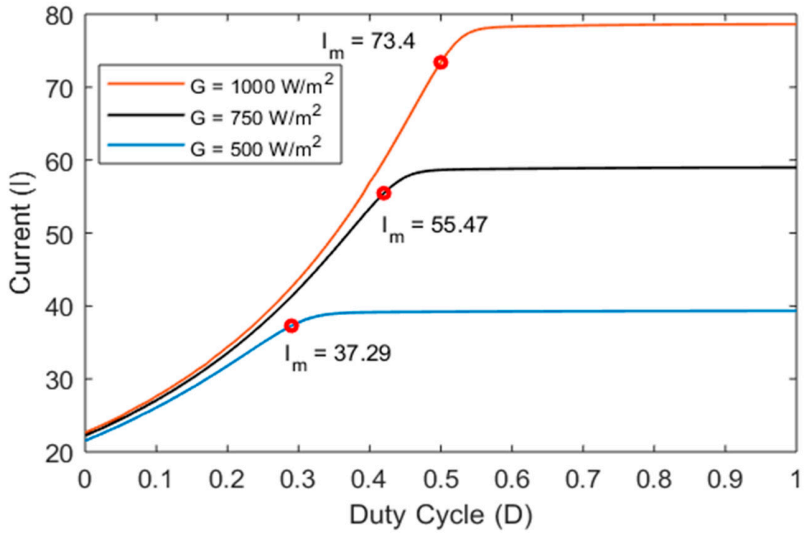
$$\Delta D_m = f\,(I_m, \Delta I_m) \tag{3}$$

The relationship $\Delta D_m = f\,(I_m,\ \Delta I_m)$ is proposed as the basis for training the NN. The NN takes I_m and ΔI_m as variables in the input layer. The NN is trained to determine the necessary variation in ΔD_m in the output layer as presented in Figure 2.

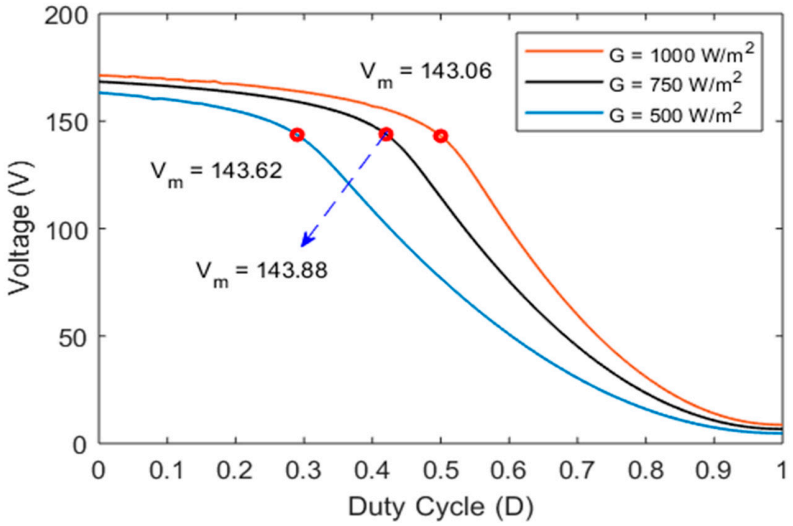


(**a**)

Figure 1. *Cont.*



(**b**)



(**c**)

Figure 1. The PV system (**a**) power, (**b**) current, and (**c**) voltage versus the duty cycle.

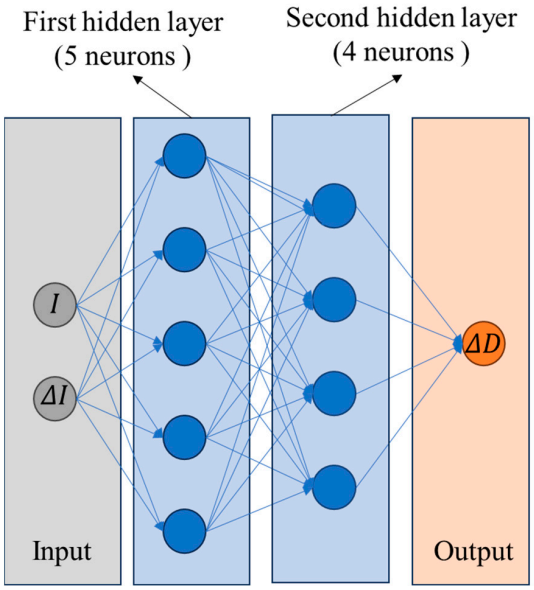


Figure 2. Neural network schematic.

2.2. Neural Network (NN) Training

A neural network (NN) tool from the MATLAB library was utilized in the current work. The neural network employed in this study is a feed-forward backpropagation neural network consisting of two hidden layers. The first layer consists of five neurons, while the second layer has four neurons. The parameters used to teach the NN are summarized in Table 2. The parameters of the NN were not optimized in the current work. Instead, the parameters were selected based on the fact that the NN of two hidden layers is capable of learning the majority of the nonlinear relations. It is important to note that the purpose of the NN in this context was to estimate the necessary ΔD_m, which was subsequently refined utilizing the P&O algorithm to achieve the optimal duty cycle. Hence, the selection of the number of neurons in the hidden layer was arbitrary.

Table 2. Characteristics of the neural network used in this work.

Parameter	Parameter Information
Type	feed-forward backpropagation
Number of hidden layers	2
Number of neurons in the first and second layer	5, 4
The inputs	(I) and (ΔI)
The output	(ΔD)

The NN was trained using a dataset consisting of 300 samples. The generation of these samples is described in Table 3. As an example, Table 3 included two representative samples. The samples were obtained theoretically by recording the parameters of the maximum power point using a Simulink model. Different values of the initial solar radiation (G) and varying values of the change in solar radiation (ΔG) were utilized for generating these samples. The values of (G) and (ΔG) were selected randomly during the process.

Table 3. Examples of data used to train the neural network.

Case	G	I	D	ΔG	ΔI	ΔD
1	75	5.89	0	$409 - 75 = 334$	$\lvert 30.38 - 5.89 \rvert = 24.49$	$\lvert 0.2105 - 0 \rvert = 0.2105$
2	409	30.38	0.2105	$619 - 409 = 210$	$\lvert 44.44 - 30.38 \rvert = 14.06$	$\lvert 0.3345 - 0.2105 \rvert = 0.124$
3	619	44.44	0.3345	-	-	-

The NN demonstrated the capacity to effectively learn the intricate relationship between I, ΔI, and ΔD_m, even when trained on a small dataset. The training process was completed in less than one second. The performance plots are given in Figure 3. The best performance was achieved with 112 iterations, as presented in Figure 3a. Figure 3b,c show the NN prediction performance for the training and validation data, each with a correlation coefficient of R greater than 0.99. The R was relatively very high, and the error was relatively very small.

The steps of building the dataset, training, and validating the NN model, and exporting the validated NN model to assist the P&O controller, are shown in Figure 4.

2.3. System Behavior

Figure 5 illustrates the system behavior at the maximum power point including the effect of the current at the maximum point (I_m) for varying (G), (ΔI_m), (ΔG), (G), and (ΔD_m). Figure 5a shows a linear relation between the solar radiation (G) and the current at the maximum point (I_m). However, Figure 5b,c show that the relation between the current (I_m), the change in current (ΔI_m), and the required change in the duty cycle (ΔD_m) is nonlinear. Hence, the utilization of an NN for mapping the inputs to outputs becomes necessary to capture these relationships.

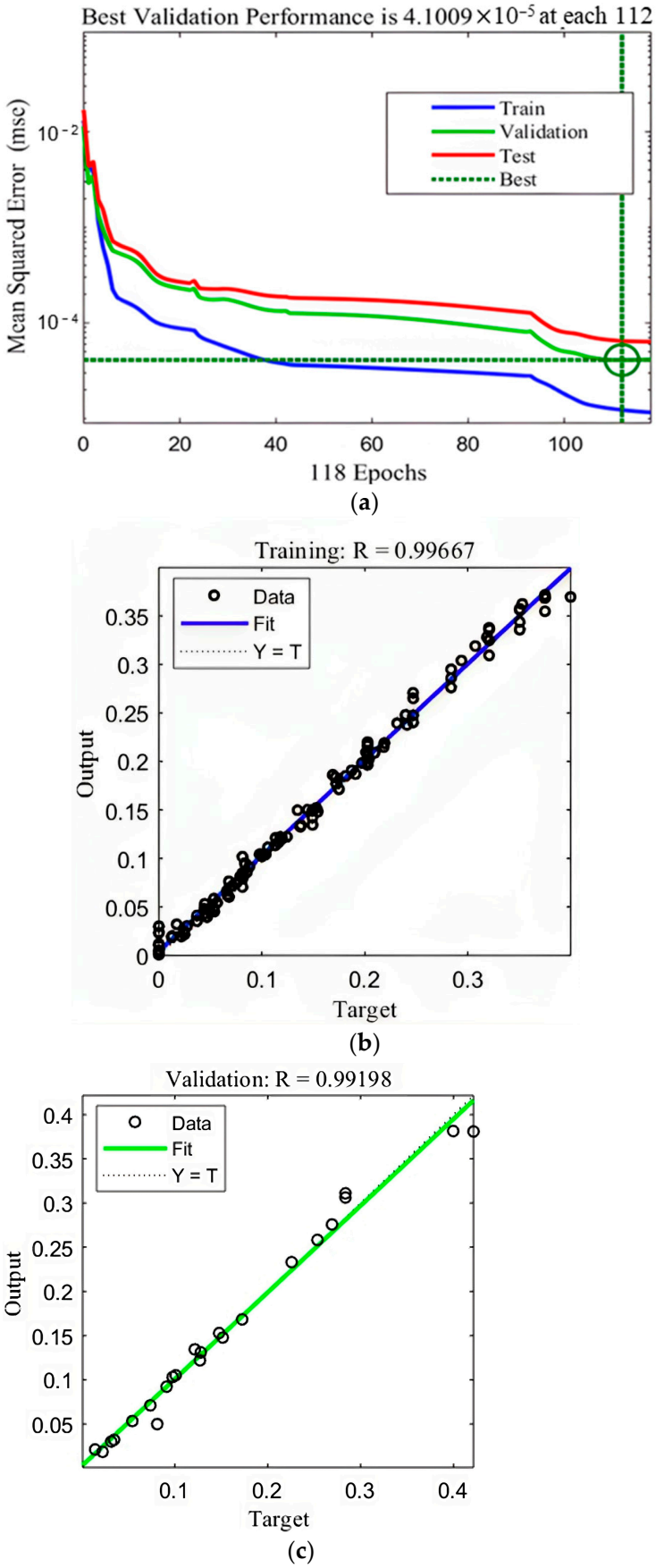


Figure 3. Performance plot of training process (**a**) NN convergence (**b**) Training data prediction (**c**) validation data prediction.

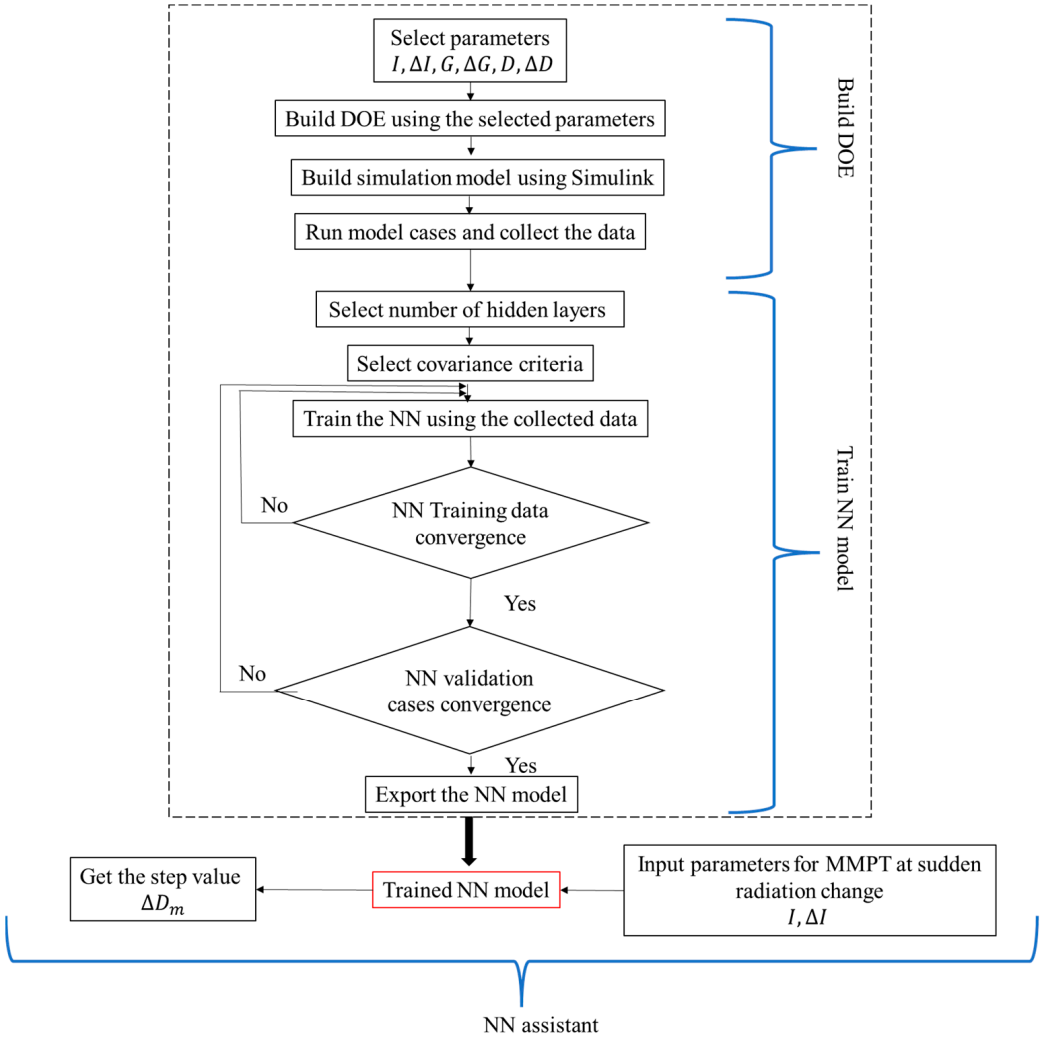
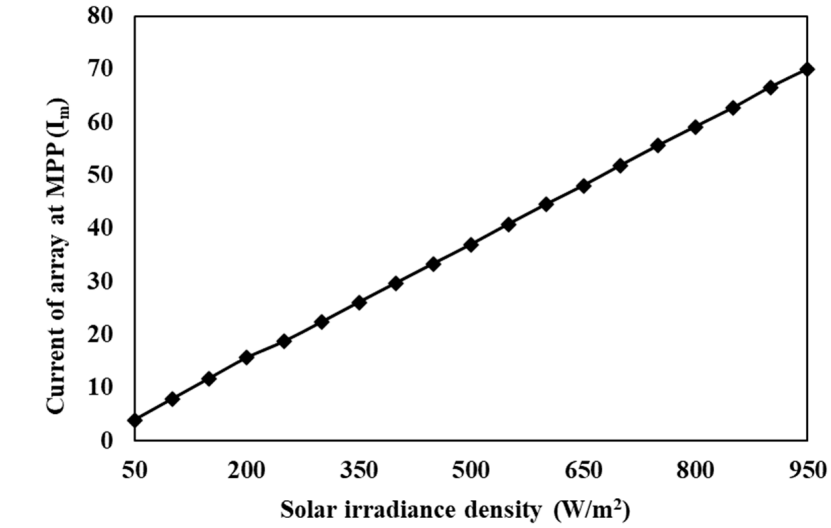


Figure 4. Neural network assistant building and training.

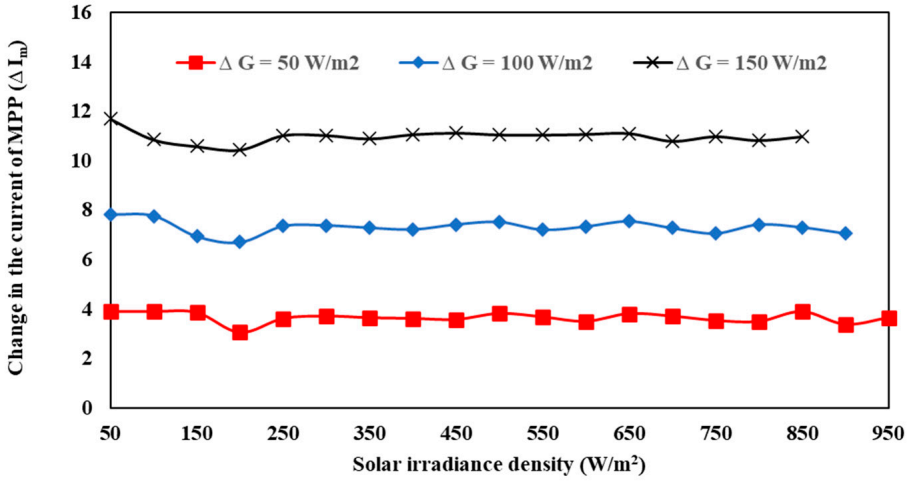
2.4. PV System Controller Design

Figure 6 represents the Simulink model for the PV system utilized in the simulation. The specifications of the PV array, the PWM generator, and the converter are given in Table 4. Figure 7 displays the Simulink model for the proposed P&O algorithm combined with an NN. The proposed algorithm incorporated an NN model that uses the I_m and ΔI_m readings as inputs to estimate ΔD_m at a sudden variation in solar irradiance. The current showed high changes during sudden fluctuations in solar irradiance. The proposed algorithm detected rapid changes in irradiance by continuously monitoring the change in current and eliminating the need for a dedicated solar irradiance sensor. Upon detecting a sudden change in irradiance levels, the P&O algorithm adjusted the duty cycle based on information provided by the neural network. The duty cycle was modified employing the equation:

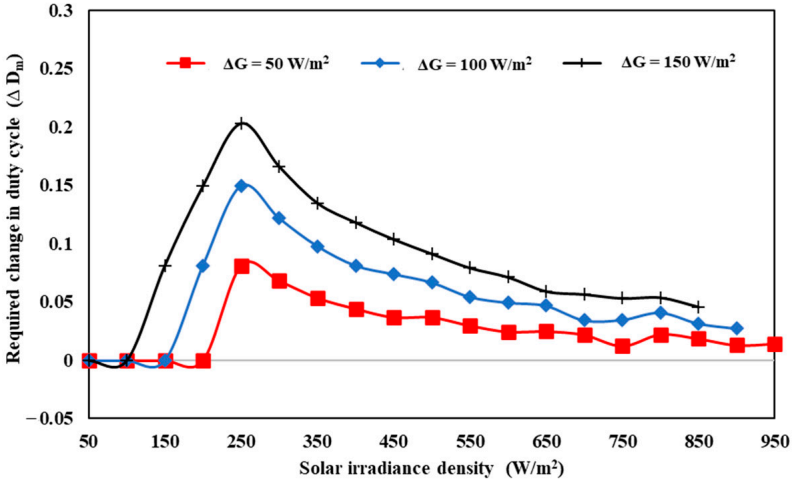
$$D = D_{old} \pm \Delta D \quad (4)$$



(**a**)



(**b**)



(**c**)

Figure 5. PV system behavior at the MPP under change in solar radiation (**a**) MPP current (**b**) MPP change in current (**c**) required duty cycle.

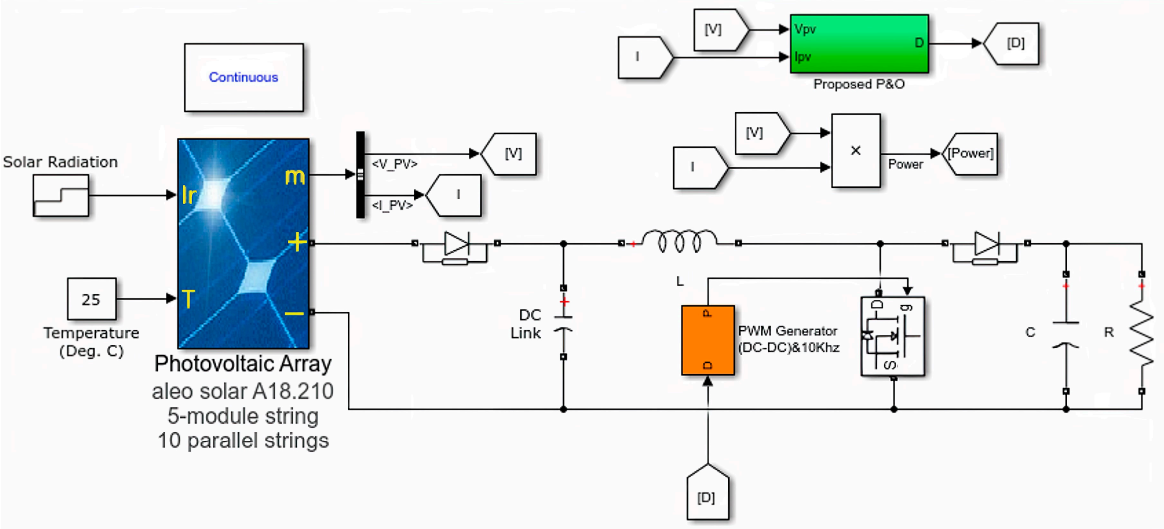


Figure 6. Simulink model for the proposed controller.

Table 4. Specifications of PV array and boost converter [74].

Parameter	Parameter Value
Array	
Series-connected modules per string	5
Parallel strings	10
Module Data	
Module	Aleo solar A18.210
Maximum power	210.16 W
Open circuit voltage V_{OC}	35.7 V
Voltage at the maximum power point V_{mp}	28.4 V
Current at the maximum power point I_{mp}	7.4 A
Short-circuit current I_{SC}	7.85 A
Number of cells per module	60
Temperature coefficient of V_{oc}	−0.34
Temperature coefficient of I_{sc}	0.041006
Boost Converter Parameters	
L	400 µH
C	50 µF
PMW adjusting frequency	10 kHz
The change in duty cycle ΔD	0.0005
The maximum duty cycle D_{max}	0.65
The minimum duty cycle D_{min}	0

The value of ΔD is typically 0.0005 in normal cases. However, ΔD will be determined using the NN when solar radiation is suddenly changed. The ΔD sign in Equation (4) was determined using the P&O algorithm, which relies on the signs of both the ΔP and ΔV. As presented in Figures 1a and 8, the P&O algorithm continuously adjusts the duty cycle in a specific direction. If the results in power increase or decrease, the P&O will adjust the operating point in the same direction by either increasing or decreasing.

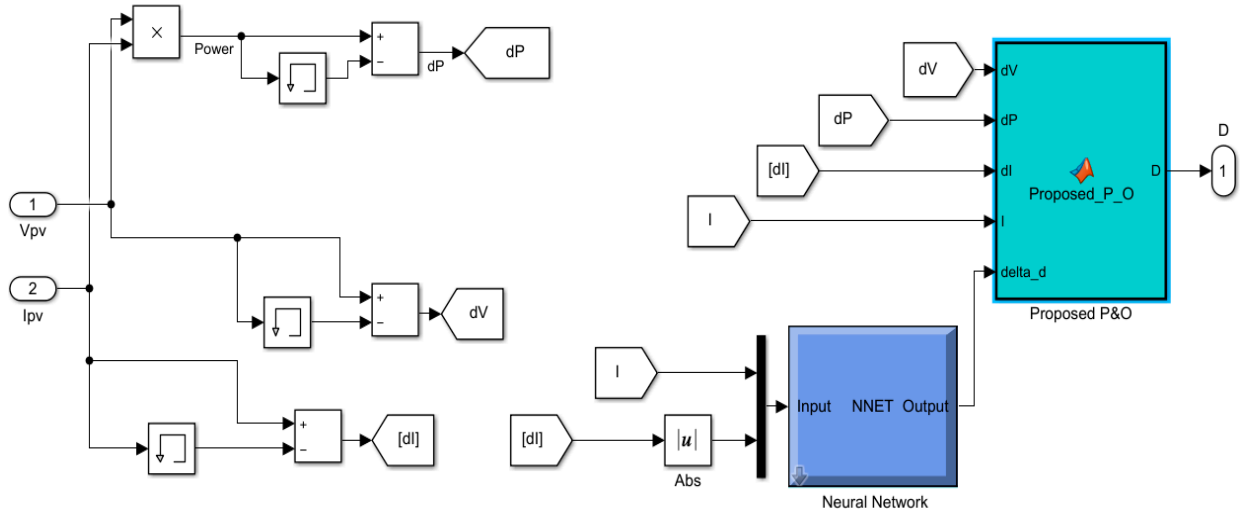


Figure 7. Integrated P&O NN controller subsystem (green box in Figure 6).

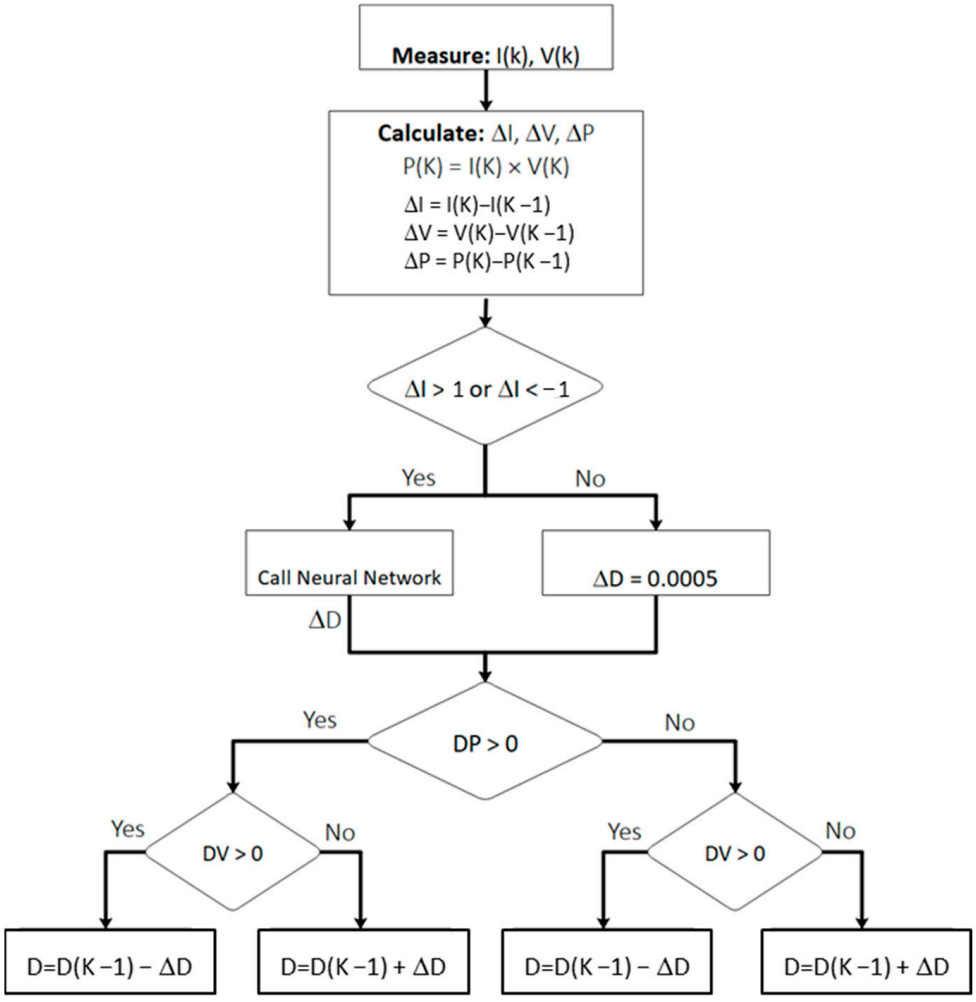


Figure 8. P&O algorithm combined with neural network.

In Figure 8, the symbols P, K, and (K − 1) refer to the power produced by the solar array, the current, and the previous measurement values, respectively. When the change in the current (ΔI) is higher than "1" or lower than "−1", the algorithm alerts the controller

that the system is experiencing a sudden change in solar irradiance. This allows the NN to promptly adjust the duty cycle in response to changing conditions.

The simulation input parameters are provided in Table 4. The input parameters used are cited from a published work by Shafi et al. [74].

3. Result and Discussion

The proposed controller was tested under various scenarios with sudden changes in solar radiation. An analysis with the conventional Perturb and Observe (P&O) algorithm is presented in Figures 9–17. The findings emphasize the enhanced performance of the proposed controller, especially in its quick responsiveness to abrupt changes in solar irradiance. Compared to the traditional P&O algorithm, the proposed controller offers the following advantages:

1. Fast response. The proposed controller rapidly adjusts to variations in solar irradiance, ensuring it remains aligned with the MPP. This swift response prevents erroneous decisions regarding correct MPP tracking.
2. Lower settling time. The proposed controller achieves steady-state conditions more quickly compared to the conventional P&O algorithm. The conventional P&O algorithm initially loses track of the MPP during sudden changes in solar irradiance and requires additional time to readjust back to the correct MPP track.
3. Improved responsiveness. Compared to the traditional P&O controller, the proposed controller shows a faster response and better performance.

In Figure 9a,b, the conventional P&O algorithm shows a delay of approximately 0.15 s and 0.2 s, respectively. The controller remains slightly distant from the MPP at 1.2 and 2.4 s. In Figure 10, when sudden changes in solar radiation occur, the power output of the PV system displays oscillations when the conventional P&O algorithm is employed. The proposed controller promptly adjusts the duty cycle resulting in a more stable power profile. Similar trends are observed in Figures 11–13, where the conventional P&O algorithm also deviates from the MPP and exhibits instability.

Figure 14a shows that the conventional P&O algorithm not only deviates from the MPP between 0.6 and 0.9 s but also frequently loses the track of the MPP. In Figure 15a, the conventional P&O is fixed far away from the MPP and frequently loses the track of the MPP between 0.3 and 0.6 s. Furthermore, even after reaching a steady-state condition, the conventional P&O produces less power between 0.6 and 0.9 s, and frequently loses the MPP between 0.3 and 0.6 s, as presented in Figure 17a.

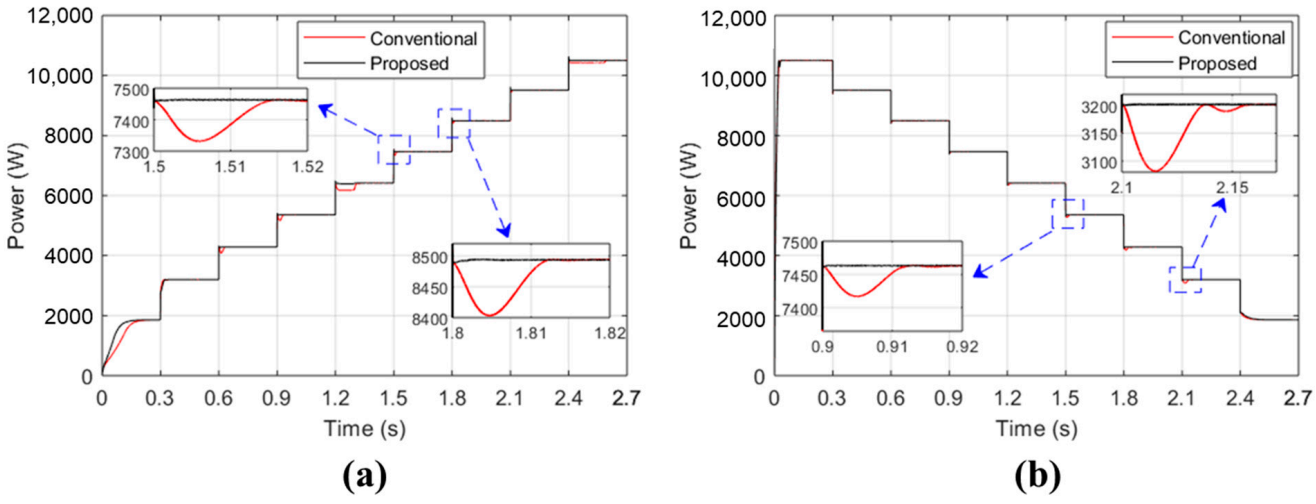


Figure 9. Performance enhancement for proposed model compared with conventional model (**a**) 100 W/m^2 increasing step each 0.3 s (**b**) 100 W/m^2 decreasing step each 0.3 s.

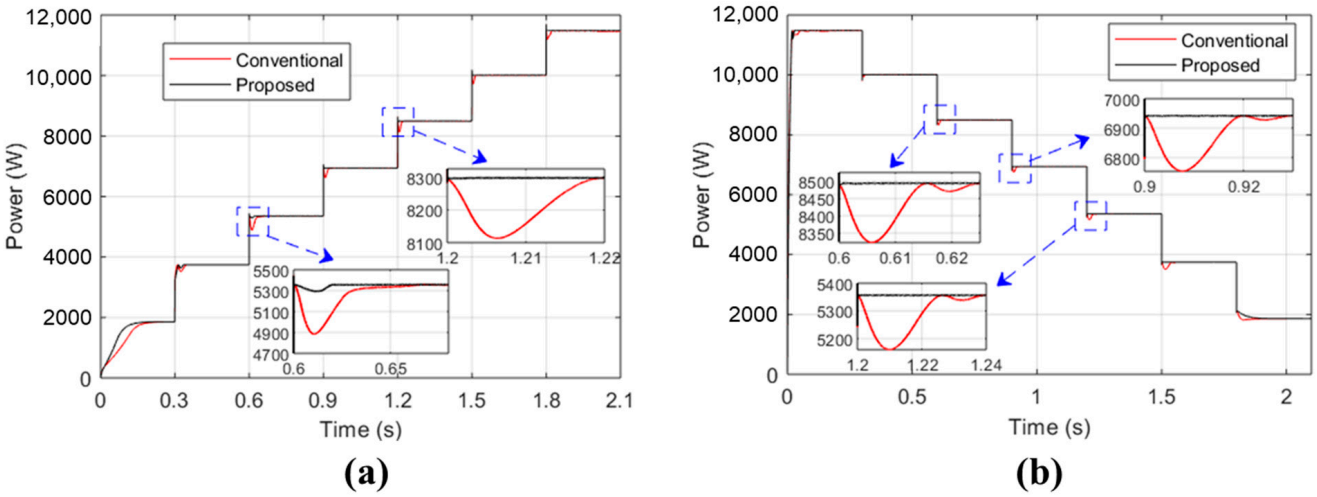


Figure 10. Performance enhancement for proposed model compared with conventional model (**a**) 150 W/m^2 increasing step each 0.3 s (**b**) 150 W/m^2 decreasing step each 0.3 s.

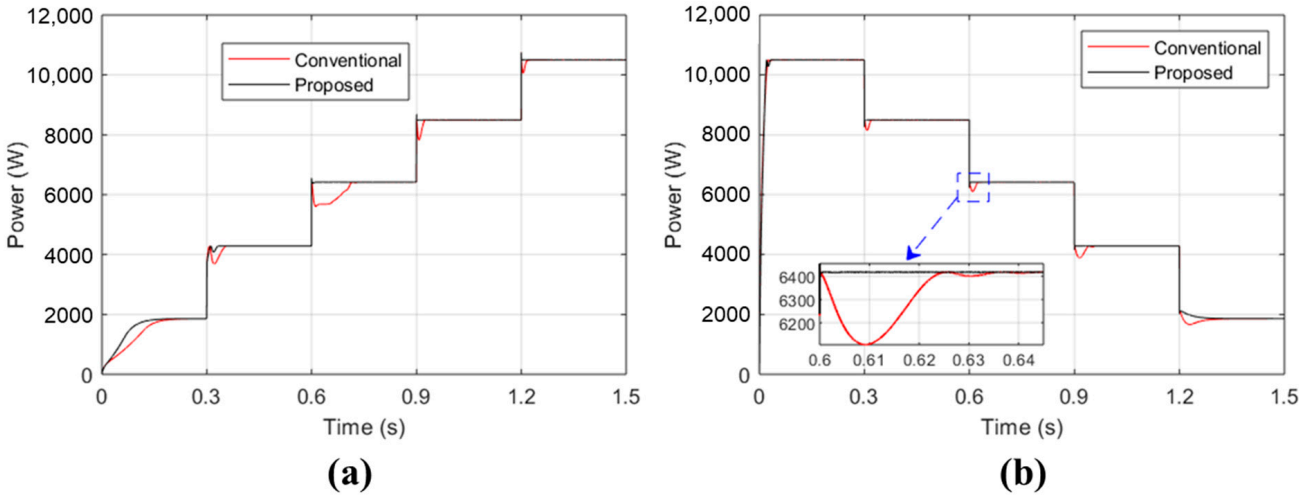


Figure 11. Performance enhancement for proposed model compared with conventional model (**a**) 200 W/m^2 increasing step each 0.3 s (**b**) 200 W/m^2 decreasing step each 0.3 s.

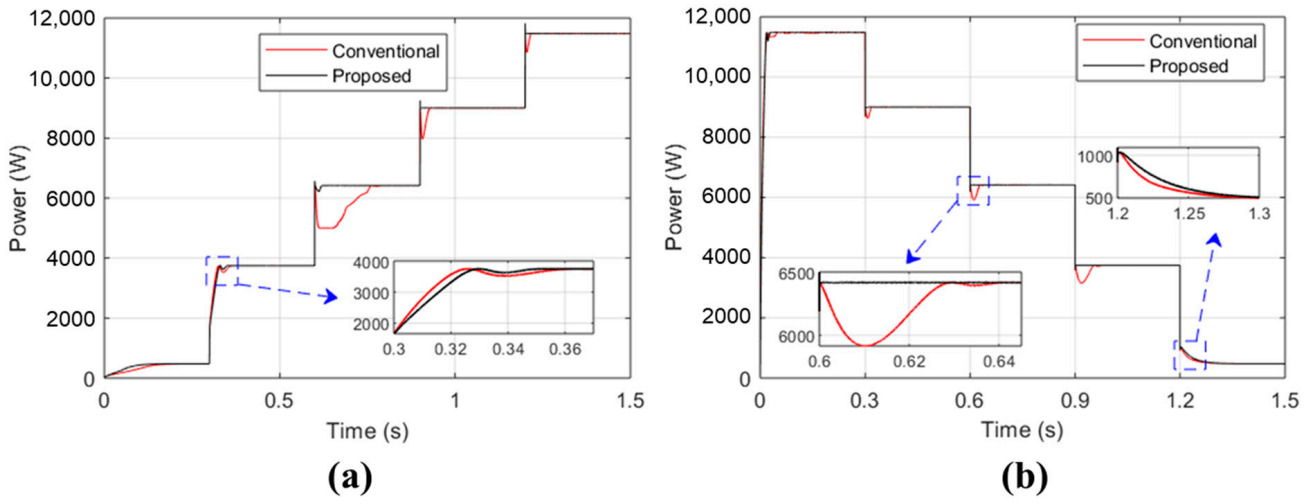


Figure 12. Performance enhancement for proposed model compared with conventional model (**a**) 250 W/m^2 increasing step each 0.3 s (**b**) 250 W/m^2 decreasing step each 0.3 s.

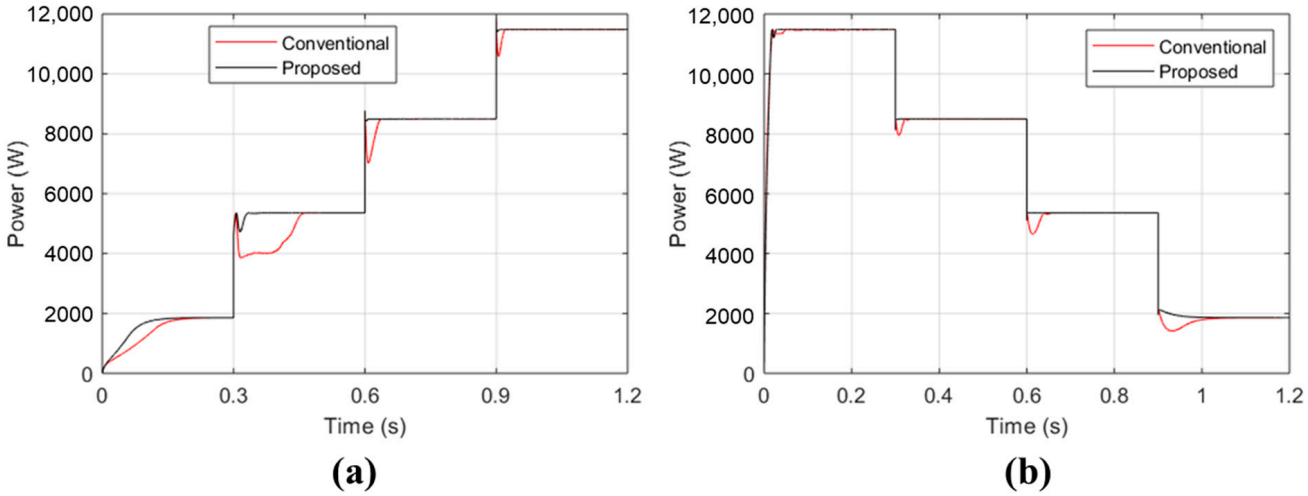


Figure 13. Performance enhancement for the proposed model compared with the conventional (**a**) 300 W/m^2 increasing step each 0.3 s (**b**) 300 W/m^2 decreasing step each 0.3 s.

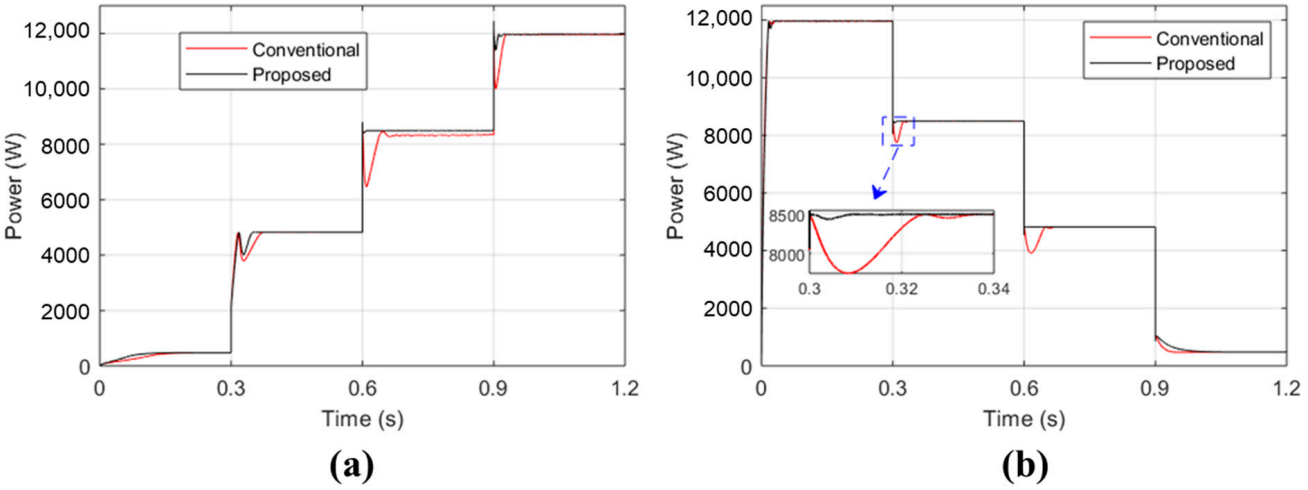


Figure 14. Performance enhancement for proposed model compared with conventional model (**a**) 350 W/m^2 increasing step each 0.3 s (**b**) 350 W/m^2 decreasing step each 0.3 s.

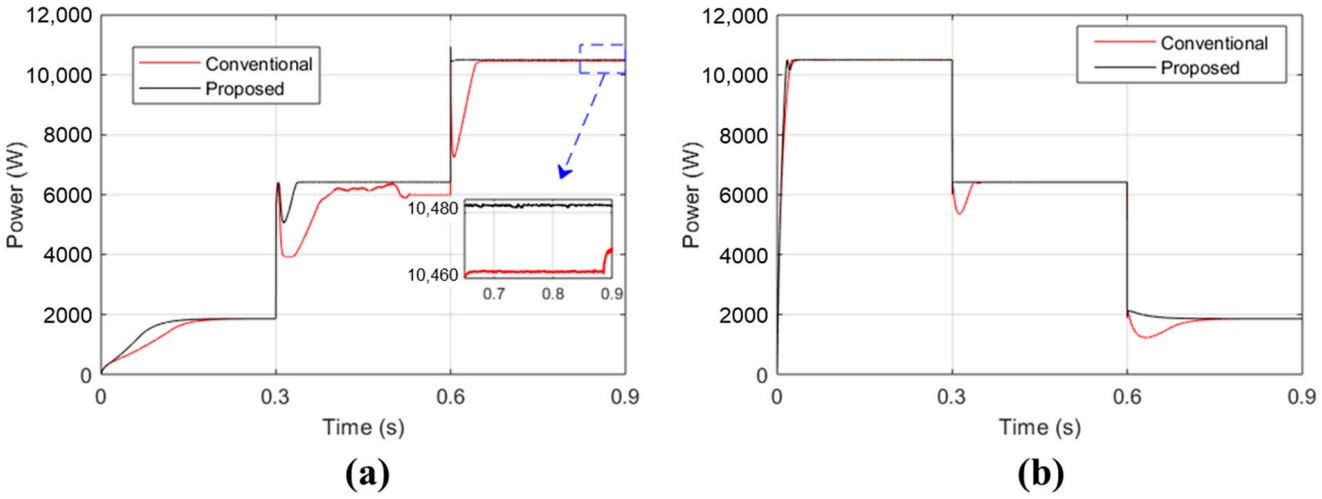


Figure 15. Performance enhancement for proposed model compared with conventional model (**a**) 400 W/m^2 increasing step each 0.3 s (**b**) 400 W/m^2 decreasing step each 0.3 s.

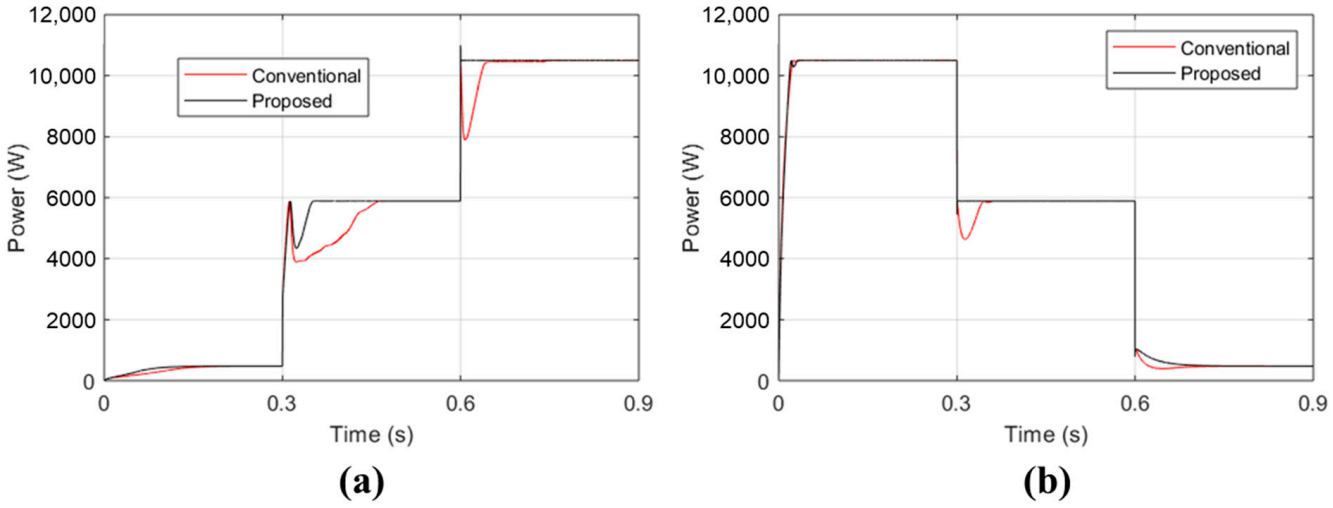


Figure 16. Performance enhancement for proposed model compared with conventional model (**a**) 450 W/m^2 increasing step each 0.3 s (**b**) 450 W/m^2 decreasing step each 0.3 s.

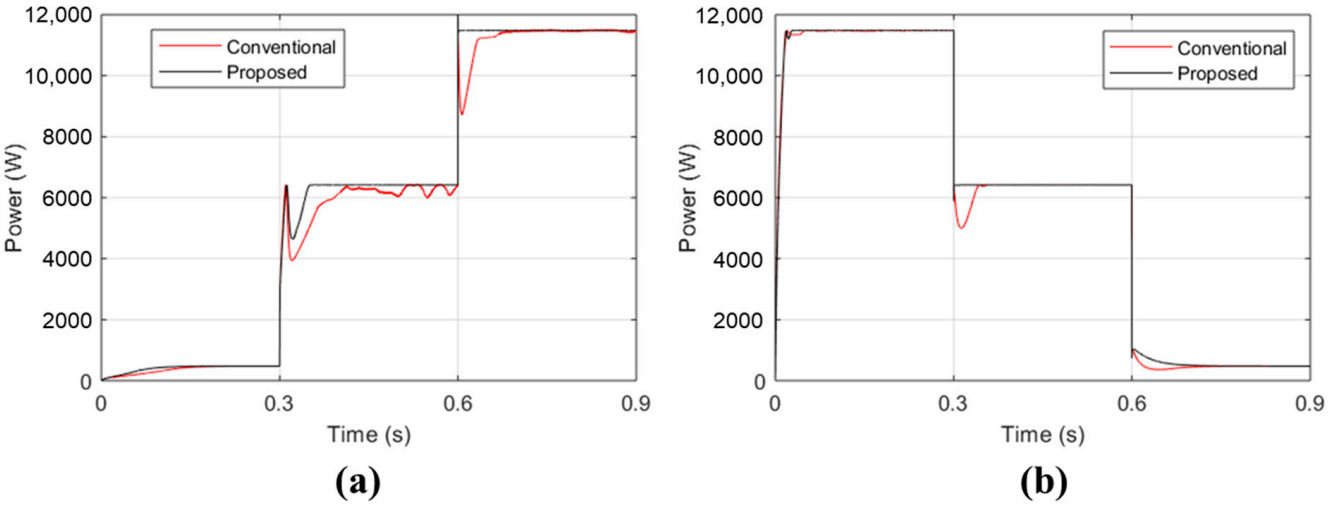


Figure 17. Performance enhancement for proposed model compared with conventional model (**a**) 500 W/m^2 increasing step each 0.3 s (**b**) 500 W/m^2 decreasing step each 0.3 s.

Figures 9–17 demonstrate that the tracking performance of the classical P&O algorithm is more adversely affected by a sudden increase in solar irradiance compared to a sudden decrease. Furthermore, the negative impact on the tracking performance of the classical P&O algorithm worsens with the increasing magnitude of changes in solar irradiance. Higher changes in solar irradiance present greater challenges for the classical P&O algorithm in maintaining accurate tracking of the maximum power point.

The results presented in Figures 9–17 demonstrate the effectiveness of the NN in estimating the required change in the duty cycle to rapidly direct the PV system towards the MPP under various situations involving sudden changes in solar irradiance. The NN serves as a good predictor that allows for accurate adjustment of the duty cycle. The NN performance shows an ability to achieve accurate duty cycle prediction even with a limited training dataset. This implies that the NN performance was not sensitive to the number of cases used to train the model and the small dataset was sufficient to make a reliable duty cycle estimator. Consequently, the overall training process becomes more time and cost-efficient.

Figure 18 presents the duty cycle over time for both the conventional P&O and the proposed controllers, capturing the scenario where the PV system experiences a sudden increase of 400 W/m^2 in solar irradiance. Figure 19 illustrates the corresponding current and its variation for the same situation. It shows that the current significantly changes in response to the sudden change in solar irradiance. At 0.3 s, the solar irradiance suddenly rises by 400 W/m^2 and the current suddenly changes by approximately 32 amperes. In Figure 19a the current drops for a while, and the change in current is very small in Figure 19b after 0.3 s. This is attributed to the high frequency of the PMW generator, which was set at 10 kHz in the proposed study. As a result, the change in current between consecutive sensor readings became very small. As per theoretical considerations, the number of readings (20,000) was twice the frequency of the PWM generator (10,000) in continuous control mode.

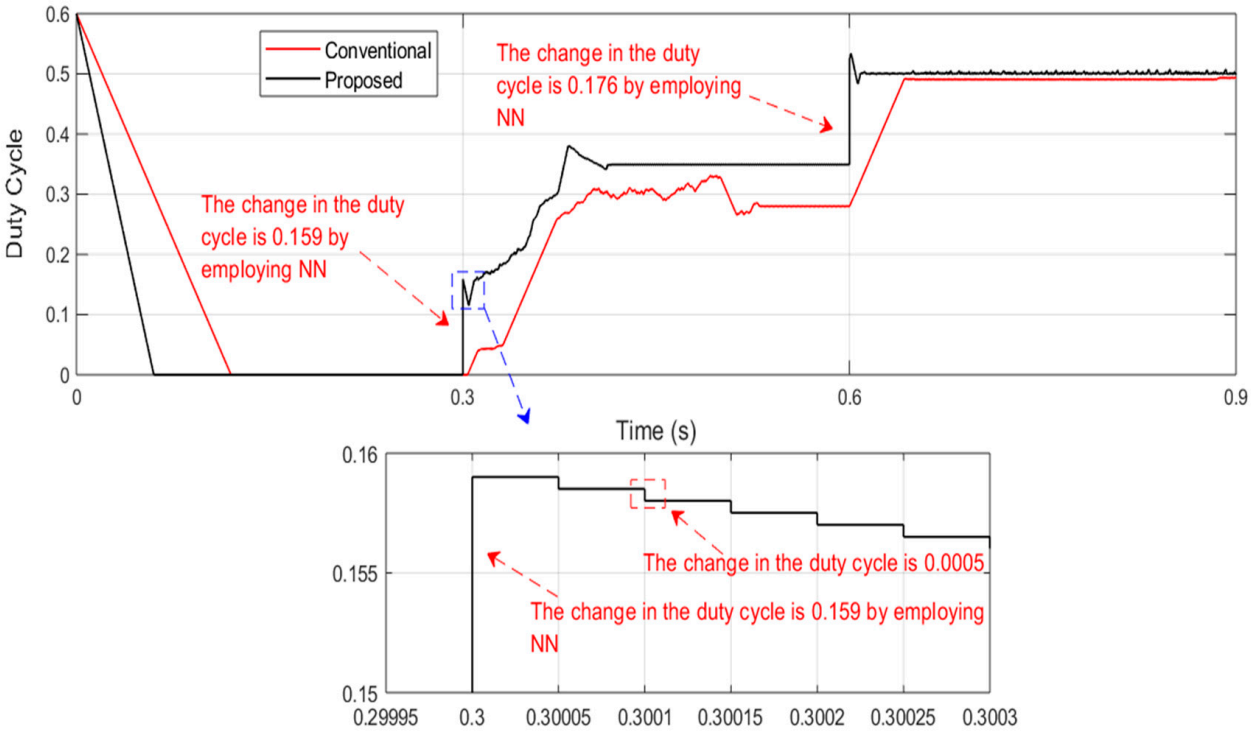


Figure 18. Comparisons for duty cycle between proposed and conventional models under 400 W/m^2 increasing step each 0.3 s.

As depicted in Figure 18, the proposed controller demonstrates the ability to adjust the duty cycle rapidly in response to a sudden change in solar irradiance. At 0.3 s, the proposed controller achieves a one-step duty cycle adjustment of 0.159 which is a rapid response compared to the conventional P&O algorithm. Consequently, the proposed controller continues to adjust the duty cycle using a fixed step size of 0.0005, similar to the conventional P&O algorithm. At 0.6 s, the proposed controller makes a one-step duty cycle adjustment of 0.176. This influential adjustment enables the system to quickly be aligned with the maximum available power to ensure efficient operation.

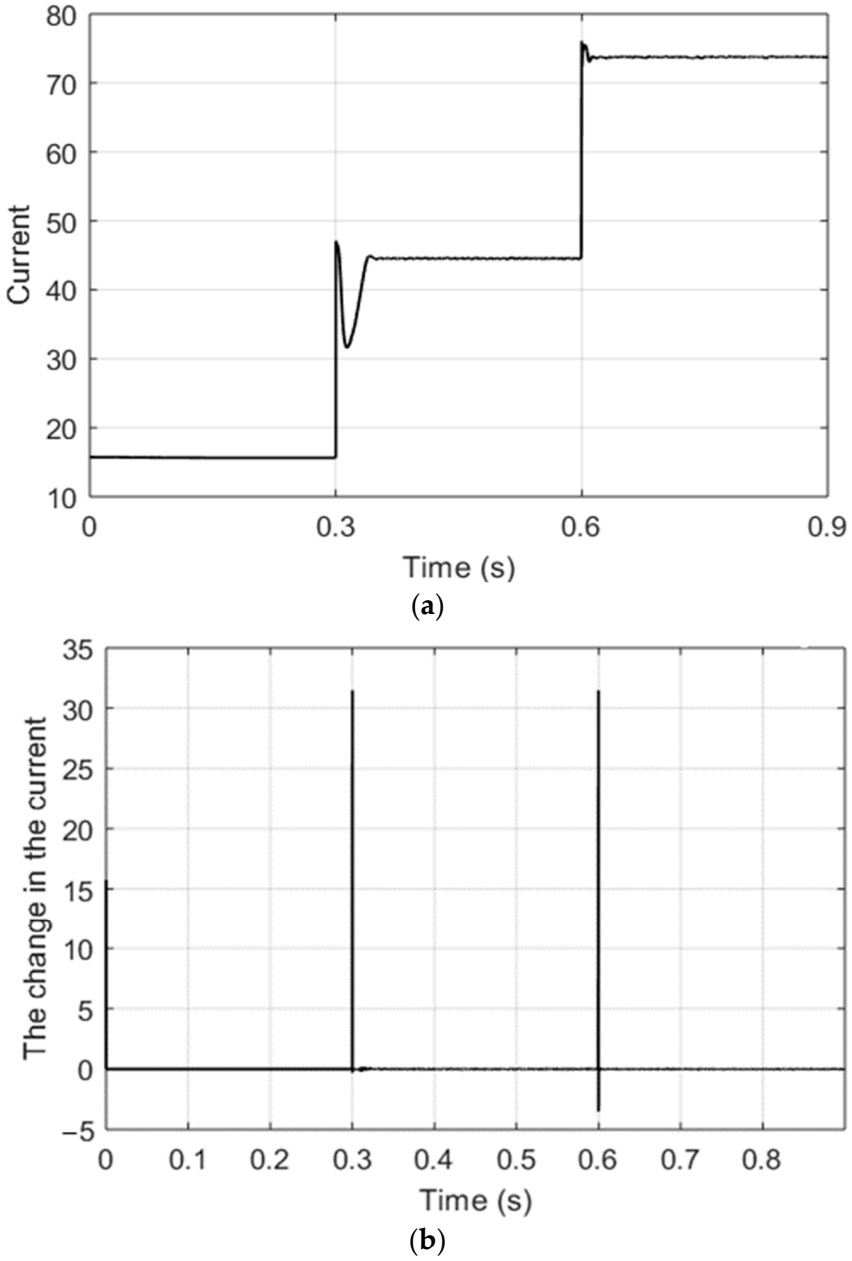


Figure 19. (**a**) Current under 400 W/m^2 increasing step each 0.3 s, (**b**) change in current under 400 W/m^2 increasing step each 0.3 s.

4. Future Work and Design Challenges

Future work will aim to explore the use of an NN to estimate the required duty cycle in the case of a gradual change in solar irradiance. The current high-frequency operation of the controller (10 kHz) poses challenges in detecting subtle changes in irradiance/current. Figure 19a shows a gradual change in current immediately after 0.3 s, but Figure 19b demonstrates that the tracking algorithm failed to capture this change. Future work will focus on upgrading neural networks to be capable of detecting and responding to gradual changes, thereby improving the algorithm's performance and overall system efficiency. This problem can be addressed by generating a large dataset, and training a recurrent neural network (RNN) to capture the gradual variation in current by analyzing the time series of the current and adjusting the duty cycle accordingly.

5. Conclusions

The Perturb and Observation (P&O) MPPT algorithm is widely utilized in commercial PV systems to maximize electrical energy production. However, the conventional P&O algorithm lacks responsiveness when faced with rapid changes in solar irradiance. This study introduces a novel approach by integrating a neural network into the P&O algorithm to enhance its tracking performance during sudden variations in solar irradiance. The NN enables rapid updates to the duty cycle in response to sudden changes in irradiance. The improved proposed algorithm demonstrates significant advantages compared with the classical P&O method. The modified algorithm exhibits exceptional speed and remains unaffected by sudden changes in irradiance, effectively avoiding confusion and preventing deviation from the maximum power point (MPP). The NN serves as an efficient estimator, eliminating the need for costly training as it was successfully trained using a small theoretical dataset.

Overall, the proposed modified algorithm, enhanced by integrating an NN, shows great promise in improving the tracking performance of PV systems under dynamic solar irradiance conditions. Its rapid response time, resistance to inaccuracies, and consistent alignment with the MPP underscore its potential to boost the overall efficiency and reliability of commercial PV systems.

Author Contributions: Software, H.S.; Writing—original draft, H.S. and A.D.; Writing—review & editing, A.D. and S.K.; Visualization, A.D. All authors have read and agreed to the published version of the manuscript.

Funding: This research received no external funding.

Institutional Review Board Statement: Not applicable.

Informed Consent Statement: Not applicable.

Data Availability Statement: The data presented in this study are available on request from corresponding author.

Conflicts of Interest: The authors declare no conflict of interest.

Nomenclature

ANFIS	Adaptive network-based fuzzy
D	Duty cycle
D_m	The duty cycle of the maximum power point
G	Solar radiation
GA	Genetic algorithm
GMPP	Global maximum power point
I	Current
I_m	Current at the maximum power point
MPP	Maximum power point
MPPT	Maximum power point tracking
NN	Neural network
P	Power
PV	Photovoltaic
P&O	Perturb and observation
T	Cell temperature
T_a	Ambient temperature
V	Voltage
V_m	Voltage at the maximum power point
V_{MPP}	Voltage at the maximum power point

References

1. Ahmed, J.; Salam, Z. An improved perturb and observe (P&O) maximum power point tracking(MPPT) algorithm for higher efficiency. *Appl. Energy* **2015**, *150*, 97–108. [CrossRef]
2. Loukriz, A.; Haddadi, M.; Messalti, S. Simulation and experimental design of a new advanced variable stepsize Incremental Conductance MPPT algorithm for PV systems. *ISA Trans.* **2016**, *62*, 30–38. [CrossRef] [PubMed]
3. Abdel-Salama, M.; El-Mohandesa, M.-T.; Goda, M. An improved perturb-and-observe based MPPT method for PV systems undervarying irradiation levels. *Sol. Energy* **2018**, *171*, 547–561. [CrossRef]
4. Killi, M.; Samanta, S. Modified Perturb and Observe MPPT Algorithm for Drift Avoidance in Photovoltaic Systems. *IEEE Trans. Ind. Electron.* **2015**, *62*, 5549–5559. [CrossRef]
5. Harrag, A.; Messalti, S. Variable step size modified P&O MPPT algorithm using GA-based hybrid of fl ine/online PID controller. *Renew. Sustain. Energy Rev.* **2015**, *49*, 1247–1260. [CrossRef]
6. Chen, P.-C.; Chen, P.-Y.; Liu, Y.-H.; Chen, J.-H.; Luo, Y.-F. A comparative study on maximum power point tracking techniques for photovoltaic generation systems operating under fast changing environments. *Sol. Energy* **2015**, *119*, 261–276. [CrossRef]
7. Ahmed, S.; Azar, A.T. Adaptive fractional tracking control of robotic manipulator using fixed-time method. *Complex Intell. Syst.* **2023**, 1–14. [CrossRef]
8. Ahmed, S.; Azar, A.T.; Tounsi, M.; Ibraheem, I.K. Adaptive Control Design for Euler–Lagrange Systems Using Fixed-Time Fractional Integral Sliding Mode Scheme. *Fractal Fract.* **2023**, *7*, 712. [CrossRef]
9. Ahmed, S.; Azar, A.T.; Tounsi, M.; Anjum, Z. Trajectory Tracking Control of Euler–Lagrange Systems Using a Fractional Fixed-Time Method. *Fractal Fract.* **2023**, *7*, 355. [CrossRef]
10. Li, X.; Wen, H.; Jiang, L.; Xiao, W.; Du, Y.; Zhao, C. An Improved MPPT Method for PV System With Fast-Converging Speed and Zero Oscillation. *IEEE Trans. Ind. Appl.* **2016**, *52*, 5051–5064. [CrossRef]
11. Metry, M.; Shadmand, M.B.; Balog, R.S.; Abu-Rub, H. MPPT of Photovoltaic Systems Using Sensorless Current-Based Model Predictive Control. *IEEE Trans. Ind. Appl.* **2017**, *53*, 1157–1167. [CrossRef]
12. Fathabadi, H. Novel fast dynamic MPPT (maximum power point tracking) technique with the capability of very high accurate power tracking. *Energy* **2016**, *94*, 466–475. [CrossRef]
13. Mohanty, S.; Subudhi, B.; Member, S.; Ray, P.K. A New MPPT Design Using Grey Wolf Optimization Technique for Photovoltaic System Under Partial Shading Conditions. *IEEE Trans. Sustain. Energy* **2016**, *7*, 181–188. [CrossRef]
14. Mohanty, S.; Subudhi, B.; Member, S.; Ray, P.K. A Grey Wolf-Assisted Perturb & Observe MPPT Algorithm for a PV System. *IEEE Trans. Energy Convers.* **2017**, *32*, 340–347. [CrossRef]
15. Sundareswaran, K.; Vignesh, V.; Palani, S. Application of a combined particle swarm optimization and perturb and observe method for MPPT in PV systems under partial shading conditions. *Renew. Energy* **2015**, *75*, 308–317. [CrossRef]
16. Rezk, H.; Fathy, A.; Abdelaziz, A.Y. A comparison of di ff erent global MPPT techniques based on meta-heuristic algorithms for photovoltaic system subjected to partial shading conditions. *Renew. Sustain. Energy Rev.* **2017**, *74*, 377–386. [CrossRef]
17. Pal, R.S.; Mukherjee, V. Metaheuristic based comparative MPPT methods for photovoltaic technology under partial shading condition. *Energy* **2020**, *212*, 118592. [CrossRef]
18. Mirza, A.F.; Mansoor, M.; Zhan, K.; Ling, Q. High-efficiency swarm intelligent maximum power point tracking control techniques for varying temperature and irradiance. *Energy* **2021**, *228*, 120602. [CrossRef]
19. Valenciaga, F.; Inthamoussou, F.A. A novel PV-MPPT method based on a second order sliding mode gradient observer. *Energy Convers. Manag.* **2018**, *176*, 422–430. [CrossRef]
20. Kihal, A.; Krim, F.; Laib, A.; Talbi, B.; Afghoul, H. An improved MPPT scheme employing adaptive integral derivative sliding mode control for photovoltaic systems under fast irradiation changes. *ISA Trans.* **2019**, *87*, 297–306. [CrossRef] [PubMed]
21. Kulaksız, A.A.; Akkaya, R. A genetic algorithm optimized ANN-based MPPT algorithm for a stand-alone PV system with induction motor drive. *Sol. Energy* **2012**, *86*, 2366–2375. [CrossRef]
22. Amrouche, B.; Belhamel, M.; Guessoum, A. Artificial intelligence based P&O MPPT method for photovoltaic systems. In *Revue des Energies Renouvelables ICRESD-07 Tlemcen*. 2007, pp. 11–16. Available online: https://www.cder.dz/download/ICRESD07_3.pdf (accessed on 12 December 2023).
23. Messalti, S.; Harrag, A.G. A New Neural Networks MPPT controller for PV Systems. In Proceedings of the IREC2015 The Sixth International Renewable Energy Congress, Sousse, Tunisia, 24–26 March 2015; pp. 1–6. [CrossRef]
24. Bendib, B.; Krim, F.; Belmili, H.; Almi, M.F.; Boulouma, S. Advanced Fuzzy MPPT Controller for a stand-alone PV system. *Energy Procedia* **2014**, *50*, 383–392. [CrossRef]
25. Bayrak, G. An improved step-up converter with a developed real-time fuzzy-based MPPT controller for PV-based residential applications. *Int. Trans. Electr. Energy Syst.* **2019**, *29*, e12140. [CrossRef]
26. Anwer, A.M.O.; Omar, F.A.; Kulaksiz, A.A. Design of a Fuzzy Logic-based MPPT Controller for a PV System Employing Design of a Fuzzy Logic-based MPPT Controller for a PV System Employing Sensorless Control of MRAS-based PMSM. *Int. J. Control. Autom. Syst.* **2020**, *18*, 2788–2797. [CrossRef]
27. Hassan, T.U.; Abbassi, R.; Jerbi, H.; Mehmood, K.; Tahir, M.F.; Cheema, K.M.; Elavarasan, R.M.; Ali, F.; Khan, I.A. A novel algorithm for MPPT of an isolated PV system using push pull converter with fuzzy logic controller. *Energies* **2020**, *13*, 4007. [CrossRef]

28. Dehghani, M.; Taghipour, M.; Gharehpetian, G.B.; Abedi, M. Optimized Fuzzy Controller for MPPT of Grid-connected PV Systems in Rapidly Changing Atmospheric Conditions. *J. Mod. Power Syst. Clean Energy* **2021**, *9*, 376–383. [CrossRef]
29. Haji, D.; Genc, N. Dynamic behaviour analysis of ANFIS based MPPT controller for standalone photovoltaic systems. *Int. J. Renew. Energy Res.* **2020**, *10*, 101–108.
30. Yilmaz, U.; Kircay, A.; Borekci, S. PV system fuzzy logic MPPT method and PI control as a charge controller. *Renew. Sustain. Energy Rev.* **2018**, *81*, 994–1001. [CrossRef]
31. Youssef, A.; El Telbany, M.; Zekry, A. Reconfigurable generic FPGA implementation of fuzzy logic controller for MPPT of PV systems. *Renew. Sustain. Energy Rev.* **2018**, *82*, 1313–1319. [CrossRef]
32. Messai, A.; Mellit, A.; Massi, P.A.; Guessoum, A.; Mekki, H. FPGA-based implementation of a fuzzy controller (MPPT) for photovoltaic module. *Energy Convers. Manag.* **2011**, *52*, 2695–2704. [CrossRef]
33. Larbes, C.; Cheikh, S.M.A.; Obeidi, T.; Zerguerras, A. Genetic algorithms optimized fuzzy logic control for the maximum power point tracking in photovoltaic system. *Renew. Energy* **2009**, *34*, 2093–2100. [CrossRef]
34. Messai, A.; Mellit, A.; Guessoum, A.; Kalogirou, S.A. Maximum power point tracking using a GA optimized fuzzy logic controller and its FPGA implementation. *Sol. Energy* **2011**, *85*, 265–277. [CrossRef]
35. Guenounou, O.; Dahhou, B.; Chabour, F. Adaptive fuzzy controller based MPPT for photovoltaic systems. *Energy Convers. Manag.* **2014**, *78*, 843–850. [CrossRef]
36. Al Nabulsi, A.; Dhaouadi, R. Efficiency optimization of a dsp-based standalone PV system using fuzzy logic and dual-MPPT control. *IEEE Trans. Ind. Inform.* **2012**, *8*, 573–584. [CrossRef]
37. Chin, C.S.; Neelakantan, P.; Yoong, H.P.; Teo, K.T.K. Optimatization of fuzzy based maximum power point tracking in PV system for rapidly changing solar irradiance. *Trans. Sol. Energy Plan.* **2011**, *2*, 130–137.
38. Cheng, P.C.; Peng, B.R.; Liu, Y.H.; Cheng, Y.S.; Huang, J.W. Optimization of a fuzzy-logic-control-based MPPT algorithm using the particle Swarm optimization technique. *Energies* **2015**, *8*, 5338–5360. [CrossRef]
39. Junaid, M.; Lini, K. Fuzzy logic controller-based MPPT for hybrid photo-voltaic/wind/fuel cell power system. *Neural Comput. Appl.* **2019**, *31*, 6331–6344. [CrossRef]
40. Kumar, A.; Chaudhary, P.; Rizwan, M. Development of Fuzzy Logic based MPPT controller for PV system at varying meteorological parameters. In Proceedings of the 12th IEEE International Conference Electronics, Energy, Environment, Communication, Computer, Control: (E3-C3), INDICON, New Delhi, India, 17–20 December 2015. [CrossRef]
41. Radjai, T.; Rahmani, L.; Mekhilef, S.; Gaubert, J.P. Implementation of a modified incremental conductance MPPT algorithm with direct control based on a fuzzy duty cycle change estimator using dSPACE. *Sol. Energy* **2014**, *110*, 325–337. [CrossRef]
42. Shiau, J.K.; Wei, Y.C.; Chen, B.C. A study on the fuzzy-logic-based solar power MPPT algorithms using different fuzzy input variables. *Algorithms* **2015**, *8*, 100–127. [CrossRef]
43. Saremi, M.; Pourfarzad, H.; Nemati, M. Design of a fuzzy current-sensor less maximum power point tracking algorithm for photovoltaic systems. *IET Renew. Power Gener.* **2021**, *14*, 3724–3731. [CrossRef]
44. Farajdadian, S.; Hosseini, S.M.H. Optimization of fuzzy-based MPPT controller via metaheuristic techniques for stand-alone PV systems. *Int. J. Hydrogen Energy* **2019**, *44*, 25457–25472. [CrossRef]
45. Ozdemir, S.; Altin, N.; Sefa, I. Fuzzy logic based MPPT controller for high conversion ratio quadratic boost converter. *Int. J. Hydrogen Energy* **2017**, *42*, 17748–17759. [CrossRef]
46. Zainuri, M.A.A.M.; Radzi, M.A.M.; Soh, A.C.; Rahim, N.A. Development of adaptive perturb and observe-fuzzy control maximum power point tracking for photovoltaic boost dc-dc converter. *IET Renew. Power Gener.* **2014**, *8*, 183–194. [CrossRef]
47. Liu, C.L.; Chen, J.H.; Liu, Y.H.; Yang, Z.Z. An asymmetrical fuzzy-logic-control-based MPPT algorithm for photovoltaic systems. *Energies* **2014**, *7*, 2177–2193. [CrossRef]
48. Li, X.; Wen, H.; Hu, Y.; Jiang, L. A novel beta parameter based fuzzy-logic controller for photovoltaic MPPT application. *Renew. Energy* **2019**, *130*, 416–427. [CrossRef]
49. Alajmi, B.N.; Ahmed, K.H.; Finney, S.J.; Williams, B.W. Fuzzy-Logic-Control Approach of a Modified Hill-Climbing Method for Maximum Power Point in Microgrid Standalone Photovoltaic System. *IEEE Trans. Power Electron.* **2011**, *26*, 1022–1030. [CrossRef]
50. Nabipour, M.; Razaz, M.; Seifossadat, S.G.; Mortazavi, S.S. A new MPPT scheme based on a novel fuzzy approach. *Renew. Sustain. Energy Rev.* **2017**, *74*, 1147–1169. [CrossRef]
51. Khosrojerdi, F.; Taheri, S.; Cretu, A.M. An adaptive neuro-fuzzy inference system-based MPPT controller for photovoltaic arrays. In Proceedings of the 2016 IEEE Electrical Power and Energy Conference (EPEC), Ottawa, ON, Canada, 12–14 October 2016; pp. 7–12. [CrossRef]
52. Chaouachi, A.; Kamel, R.M.; Nagasaka, K. A novel multi-model neuro-fuzzy-based MPPT for three-phase grid-connected photovoltaic system. *Sol. Energy* **2010**, *84*, 2219–2229. [CrossRef]
53. Essefi, R.M.; Souissi, M.; Abdallah, H.H. Maximum Power Point Tracking Control Using Neural Networks for Stand-Alone Photovoltaic Systems. *Int. J. Mod. Nonlinear Theory Appl.* **2014**, *2*, 53–65. [CrossRef]
54. Assahout, S.; Elaissaoui, H.; El Ougli, A.; Tidha, B.; Zrouri, H. A Neural Network and Fuzzy Logic based MPPT Algorithm for Photovoltaic Pumping System. *Int. J. Power Electron. Drive Syst.* **2018**, *9*, 1823–1833. [CrossRef]
55. Bendib, B.; Krim, F.; Belmili, H.; Almi, M.F.; Bolouma, S. An intelligent MPPT approach based on neural-network voltage estimator and fuzzy controller, applied to a stand-alone PV system. In Proceedings of the 2014 IEEE 23rd International Symposium on Industrial Electronics (ISIE), Istanbul, Turkey, 1–4 June 2014; pp. 404–409. [CrossRef]

56. Akkaya, R. DSP implementation of a PV system with GA-MLP-NN based MPPT controller supplying BLDC motor drive. *Energy Convers. Manag.* **2007**, *48*, 210–218. [CrossRef]
57. Heidari, M. Improving Efficiency of Photovoltaic System by Using Neural Network MPPT and Predictive Control of Converter. *Int. J. Renew. Energy Res.* **2019**, *6*, 1524–1529.
58. Bouselham, L.; Hajji, M.; Hajji, B.; Bouali, H. A new MPPT-based ANN for photovoltaic system under partial shading conditions. *Energy Procedia* **2017**, *111*, 924–933. [CrossRef]
59. Kassem, A.M. Electrical Power and Energy Systems MPPT control design and performance improvements of a PV generator powered DC motor-pump system based on artificial neural networks. *Int. J. Electr. Power Energy Syst.* **2012**, *43*, 90–98. [CrossRef]
60. Zazi, M.; Barradi, Y. The MPPT Control ofPV System by Using Neural Networks Based on Newton Raphson Method. In Proceedings of the 2014 International Renewable and Sustainable Energy Conference (IRSEC), Ouarzazate, Morocco, 17–19 October 2014.
61. Issaadi, S.; Issaadi, W.; Khireddine, A. New intelligent control strategy by robust neural network algorithm for real time detection of an optimized maximum power tracking control in photovoltaic systems. *Energy* **2019**, *187*, 115881. [CrossRef]
62. Chekired, F.; Mellit, A.; Kalogirou, S.A.; Larbes, C. Intelligent maximum power point trackers for photovoltaic applications using FPGA chip: A comparative study. *Sol. Energy* **2014**, *101*, 83–99. [CrossRef]
63. Dounis, A.I.; Kofinas, P.; Papadakis, G.; Alafodimos, C. A direct adaptive neural control for maximum power point tracking of photovoltaic system. *Sol. Energy* **2015**, *115*, 145–165. [CrossRef]
64. Ali, M.N.; Mahmoud, K.; Lehtonen, M. Promising MPPT Methods Combining Metaheuristic, Fuzzy-Logic and ANN Techniques for Grid-Connected Photovoltaic. *Sensors* **2021**, *21*, 1244. [CrossRef]
65. Syafaruddin; Karatepe, E.; Hiyama, T. Artificial neural network-polar coordinated fuzzy controller based maximum power point tracking control under partially shaded conditions. *IET Renew. Power Gener.* **2009**, *3*, 239–253. [CrossRef]
66. Punitha, K.; Devaraj, D.; Sakthivel, S. Artificial neural network based modified incremental conductance algorithm for maximum power point tracking in photovoltaic system under partial shading conditions. *Energy* **2013**, *62*, 330–340. [CrossRef]
67. Tsai, M.; Tseng, C.; Hong, G.; Lin, S. A Novel MPPT Control Design for PV Modules Using Neural Network Compensator. In Proceedings of the 2012 IEEE International Symposium on Industrial Electronics, Hangzhou, China, 28–31 May 2012; pp. 1742–1747.
68. Sheraz, M.; Abido, M.A. An Efficient MPPT controller Using Differential Evolution and Neural Network. In Proceedings of the EEE International Conference on Power and Energy, Kota Kinabalu, Malaysia, 2–5 December 2012; pp. 378–383.
69. Singh, M.D.; Shine, V.J.; Janamala, V. Application of Artificial Neural Networks in Optimizing MPPT Control for Standalone Solar PV System. In Proceedings of the 2014 International Conference on Contemporary Computing and Informatics (IC3I), Mysuru, India, 27–29 November 2014; pp. 162–166.
70. Hidayat, A. Short Circuit Current Based ANN MPPT For Battery Charging. In Proceedings of the 2019 International Electronics Symposium (IES), Surabaya, Indonesia, 27–28 September 2019; pp. 422–427.
71. Habibi, M.N. Hybrid Maximum Power Point Tracking Using Artificial Neural Network-Incremental Conduction with Short Circuit Current of Solar Panel. In Proceedings of the 2019 International Electronics Symposium (IES), Surabaya, Indonesia, 27–28 September 2019; pp. 63–69.
72. Zečević, Ž.; Rolevski, M. Neural Network Approach to MPPT Control and Irradiance Estimation. *Appl. Sci.* **2020**, *10*, 5051. [CrossRef]
73. Attia, H.A. High performance PV system based on artificial neural network MPPT with PI controller for direct current water pump applications. *Int. J. Power Electron. Drive Syst.* **2019**, *10*, 1329–1338. [CrossRef]
74. Shafi, A.; Sharadga, H.; Hajimirza, S. Design of optimal power point tracking controller using forecasted photovoltaic power and demand. *IEEE Trans. Sustain. Energy* **2019**, *11*, 1820–1828. [CrossRef]

Disclaimer/Publisher's Note: The statements, opinions and data contained in all publications are solely those of the individual author(s) and contributor(s) and not of MDPI and/or the editor(s). MDPI and/or the editor(s) disclaim responsibility for any injury to people or property resulting from any ideas, methods, instructions or products referred to in the content.